

JETS AS A SOURCE OF INFORMATION ABOUT PHOTON STRUCTURE *

MAREK TAŠEVSKÝ

*Institute of Physics, Academy of Sciences of the Czech Republic, Na Slovance 2
Praha, CZ - 182 21, Czech Republic*

E-mail: tasevsky@fzu.cz

On behalf of the H1 Collaboration.

ABSTRACT

A review of recent jet measurements of the photon structure from the H1 experiment at HERA is presented. A manifestation of the photon structure in single-jet and di-jet cross sections is shown. From di-jet cross sections the effective parton distribution function is extracted and its dependence on the scale as well as the photon virtuality is discussed.

1. Introduction

The photon, as an elementary particle, is considered to be structureless. And yet, from numerous experimental data it follows that in high energy $\gamma\gamma$ or γp interactions the photon behaves like a hadron, an object with a structure. Quantum mechanically, the photon can fluctuate into a fermion-antifermion pair which can further evolve in the framework of QED and QCD. This is called photon structure and it can be investigated by means of the jets. Like those of the proton, parton distribution functions (PDF) of the photon depend on the probing scale¹, but additionally also on its virtuality Q^2 . This latter dependence was measured in the single-jet study² and more recently in an H1 di-jet analysis where the effective PDF of the virtual photon was extracted for the first time.

2. Single-Jet and Di-Jet Cross Sections

For appropriately normalised matrix elements M_{ij}^{kl} and neglecting the contribution of the longitudinally polarised photons the expression for the resolved photon

^{*}To appear in the *Proceedings of the DIS98 Workshop*, held in Brussels, Belgium, April 4 - 8, 1998.

contribution to the di-jet cross section in ep collisions reads

$$\frac{d\sigma^{\text{ep}}}{dydx_\gamma dx_p d\cos\theta dQ^2} = \frac{f_{\gamma/e}(y, Q^2)}{y} \sum_{i,j,k,l} \frac{f_{i/\gamma}(x_\gamma, \mu_F^2, Q^2)}{x_\gamma} \frac{f_{j/p}(x_p, \mu_F^2)}{x_p} |M_{ij}^{kl}|^2 \quad (1)$$

where $f_{\gamma/e}$ denotes the flux of transversely polarised virtual photons inside electron, $f_{i/\gamma}, f_{j/p}$ are PDF of the photon and proton respectively taken at $x_\gamma(x_p)$, the fraction of the photon(proton) momentum carried by the parton entering the hard subprocess, and at the factorization scale μ_F . The M_{ij}^{kl} are the leading order (LO) matrix elements of the binary parton level processes $ij \rightarrow kl$, proportional to $\alpha_s(\mu_R^2)$. We assumed $\mu_F = \mu_R = E_T$ (the transverse energy of the jet).

To correct for detector, fragmentation and higher order effects, PYTHIA and HERWIG MC event generators were used for photoproduction and HERWIG, RAPGAP, ARIADNE and LEPTO for low Q^2 events. As input PDFs of the virtual photon, either the simple Drees-Godbole³ (DG) virtuality suppression factor

$$L(E_T^2, Q^2, \omega) = \frac{\ln((E_T^2 + \omega^2)/(Q^2 + \omega^2))}{\ln((E_T^2 + \omega^2)/\omega^2)}, \quad \text{with free parameter } \omega \quad (2)$$

multiplying the PDFs of the real photon (as L for quarks and L^2 for gluons) or set D of the SaS⁴ parameterisations was taken.

In Fig.1a the photoproduction di-jet cross sections are compared with next-to-leading order (NLO) calculations⁵ in which the photon PDFs were taken from F_2^γ measurements in $\gamma\gamma$ interactions at LEP (and also from PEP, PETRA and TRISTAN data). The data were corrected for detector effects by an unfolding procedure⁶. The satisfactory overall description of the di-jet ep data supports the universality of the photon parton distributions. However, the data indicate that adjustments of the PDF at high x_γ are required where no F_2^γ measurements have been made so far.

In Fig.1b the inclusive single-jet cross sections as a function of Q^2 are compared to predictions of LEPTO which contains only the direct coupling of the photon to quarks. The prediction agrees with the data well in the DIS region where, typically, $E_T^2 \ll Q^2$. However, the model cannot describe the data in the region $E_T^2 > Q^2$ where the contribution of the virtual resolved photon is expected to be important. If the same data are compared to HERWIG and RAPGAP, generators containing resolved processes, a good agreement is achieved only if the photon PDF is suppressed with increasing Q^2 . The di-jet data, on the other hand, enable to construct the distribution of x_γ — a quantity closely related to the partonic content of the photon — or more, to extract the effective parton distribution function of the photon (see section 3). In the more recent H1 di-jet analysis from which preliminary plots 2, 3a, 4 are shown, the most important cuts imposed on the data were: $E_T > 5$ GeV and $-3 < \eta < 0$ for two highest E_T jets constructed on clusters and tracks in γ^*p cms using CDF cone algorithm⁷. The results were integrated over the region of inelasticity, $0.25 < y < 0.7$, and studied in the region of the photon virtuality, $1.4 < Q^2 < 25$

GeV². The limits on E_T and Q^2 were driven by the condition $E_T^2 \gg Q^2$ — a natural requirement when investigating the virtual photon structure (see the mean values of E_T^2 and Q^2 in Fig.4). The data were corrected using the mentioned unfolding procedure⁶. The virtuality dependence of the di-jet cross sections, $d\sigma/dx_\gamma$, is shown in Fig.2. Again, the HERWIG and RAPGAP models incorporating a resolved photon contribution with a virtuality-dependent suppression, describe the data satisfactorily. In Fig.3a, the ratio of resolved to direct contributions, defined as $\sigma(x_\gamma \leq 0.75)/\sigma(x_\gamma > 0.75)$ is plotted as a function of Q^2 . The data in Figs.2 and 3a are compatible with DG virtuality suppression for $0.05 \leq \omega \leq 0.1$ GeV.

3. Effective Parton Distribution of the Photon

The concept of effective PDF was developed for jet analyses at CERN SPS⁸ where it was not possible to distinguish the contributions of individual subprocesses $ij \rightarrow kl$ to the sum in Eq. (1). Applied to ep collisions at HERA, this approach allows us to approximate the formula (1) by a simple product

$$\frac{d\sigma^{\text{ep}}}{dy dx_\gamma dx_p d\cos\theta dQ^2} \approx \frac{f_{\gamma/e}(y, Q^2)}{y} \frac{f_{\text{eff}}^\gamma(x_\gamma, E_T^2, Q^2)}{x_\gamma} \frac{f_{\text{eff}}^p(x_p, E_T^2)}{x_p} |M_{SES}|^2 \quad (3)$$

of a *single effective subprocess* matrix element M_{SES} and the *effective PDF* of the colliding photon and proton

$$f_{\text{eff}}^{\gamma/p}(x, E_T^2, Q^2) = \sum_i^{n_f} [q_i(x, E_T^2, Q^2) + \bar{q}_i(x, E_T^2, Q^2)] + \frac{9}{4} g(x, E_T^2, Q^2). \quad (4)$$

The measured di-jet cross sections were corrected to the LO di-parton cross section by the unfolding procedure⁶. The effective PDF of the photon f_{eff}^γ was then determined by comparing the measured di-parton cross section with that calculated by MC model using the GRV-LO photon PDF and incorporating, for the virtual photon, the DG suppression factor:

$$f_{\text{eff}}^{\gamma, \text{DATA}}(x_\gamma, E_T^2, Q^2) = f_{\text{eff}}^{\gamma, \text{GRV-LO}}(x_\gamma, E_T^2, Q^2) L(E_T^2, Q^2, \omega^2) \frac{d\sigma^{\text{DATA}}/dx_\gamma}{d\sigma^{\text{MC, GRV-LO}}/dx_\gamma} \quad (5)$$

In Fig.3b the effective PDF of the (almost) real photon integrated over the range $0.4 < x_\gamma < 0.7$ is shown as a function of the scale E_T^2 . In this x_γ region f_{eff}^γ is dominated by the quarks. Also shown are the PDFs from GRV-LO parameterisations of the photon⁹, which is in good agreement with the data, and of the pion¹⁰, which differs from measurement both in shape and absolute rate. The increase of f_{eff}^γ with E_T^2 seen in the data is compatible with a logarithmic dependence of q^γ on μ_F , which is expected from the inhomogeneous term in the DGLAP evolution equation. In Fig.4 the effective PDF of the virtual photon is presented in four Q^2 intervals and compared

with the predictions of GRV-LO (for $\omega = 0.05$ and 0.1 GeV) and with SaS1D and SaS2D parameterisations. The data are in good agreement with the GRV for both values of ω , the SaS parameterisations tend to fall more rapidly in the low x_γ region than the data.

4. Conclusion

New kinematical regions were explored by the H1 experiment in single-jet and di-jet analyses. From photoproduction data the scale dependence of the photon effective PDF was determined. The observed logarithmic increase agrees with the prediction of perturbative QCD. The low Q^2 data indicate the importance of the resolved photon contribution to the total jet cross section and its suppression with increasing virtuality. The Q^2 dependence of the di-jet cross section and of the ratio $\sigma^{res}/\sigma^{dir}$ was shown. The first measurements of the LO effective PDF of the photon in the region $1.4 < Q^2 < 25$ GeV² was presented.

5. Acknowledgements

I thank J. Chýla and S. Maxfield for the reading of the text and for comments. This work is supported by the Grant Agency of Academy of Sciences of the Czech Republic under the grant no. A1010821, by the Grant Agency of the Czech Republic under the grant no. 202/96/0214 and by the Grant Agency of Charles University under the grant number 177.

6. References

1. H1 Collab., C. Adloff et al., *Eur. Phys. J. C* **1**, 97 (1998)
2. H1 Collab., C. Adloff et al., *Phys. Lett. B* **415**, 418 (1997)
3. M. Drees and R.M. Godbole, *Phys. Rev. D* **50**, 3124 (1994)
4. G.A. Schuler, T. Sjöstrand *Phys. Lett. B* **376**, 193 (1996)
5. M. Klasen and G. Kramer, DESY-96-246, hep-ph/9611450 (1996),
Z. Phys. C **76**, 67 (1997)
6. G. D'Agostini, *Nucl. Instrum. Methods A* **362**, 487 (1995)
7. code written by L. del Pozo and modified by M. Seymour.
8. B.L. Combridge and C.J. Maxwell, *Nucl. Phys. B* **239**, 429 (1984)
9. M. Glück, E. Reya, and A. Vogt *Z. Phys. C* **53**, 127 (1992)
10. M. Glück, E. Reya, and A. Vogt *Z. Phys. C* **53**, 651 (1992)

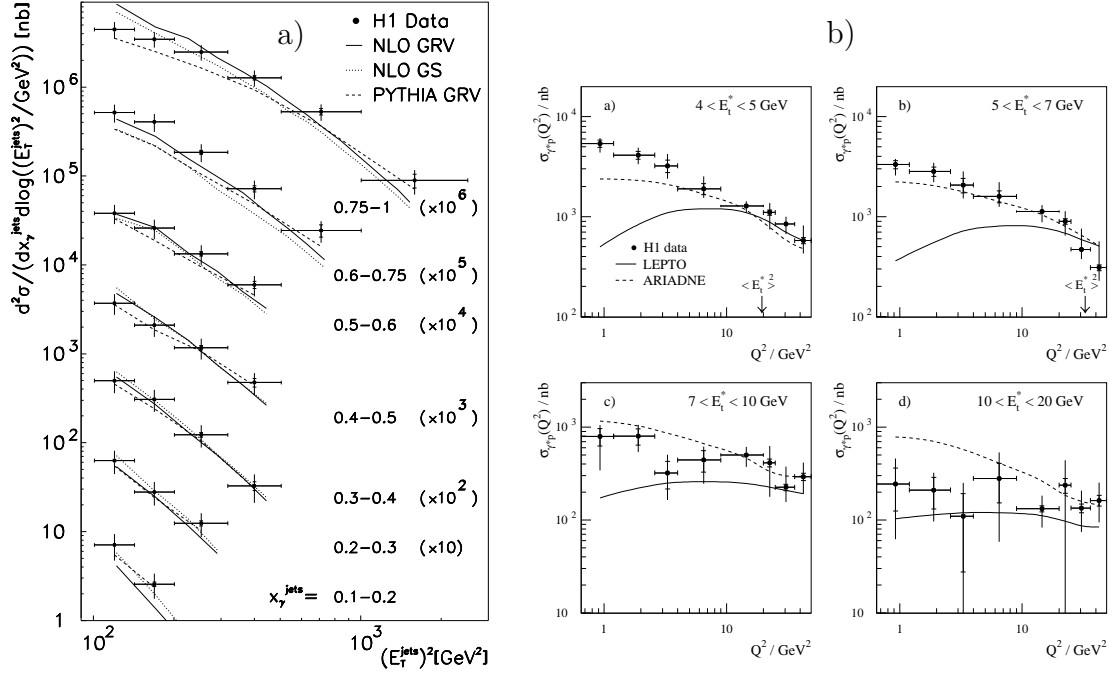


Figure 1: a) The photoproduction di-jet cross section as a function of $(E_T^{jets})^2$ and x_γ^{jets} in the range $0.2 < y < 0.83$. The data (full circles) are compared to the PYTHIA with the GRV-LO photon PDF (dashed curve) and to analytical NLO calculations⁵ with GRV-HO (full line) and GS96 (dotted line) photon PDF. b) The inclusive γ^*p single-jet cross section as a function of Q^2 in the range $0.3 < y < 0.6$. The data (full points) are compared to LEPTO (solid line) and ARIADNE (dashed line).

H1 Preliminary

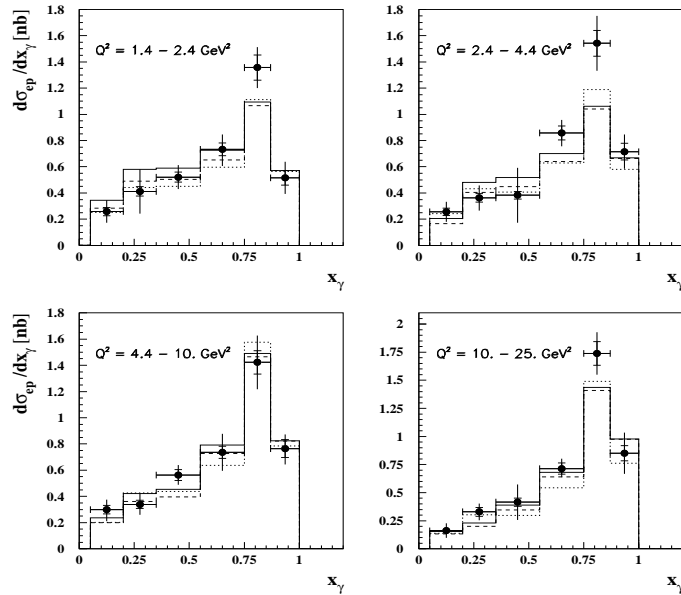


Figure 2: The differential di-jet ep cross sections as a function of x_γ in four Q^2 intervals (points) compared to HERWIG with $\omega = 0.1, 0.05 \text{ GeV}$ (full, dashed line resp.) and RAPGAP with $\omega = 0.1 \text{ GeV}$ (dotted line) used in DG suppression function.

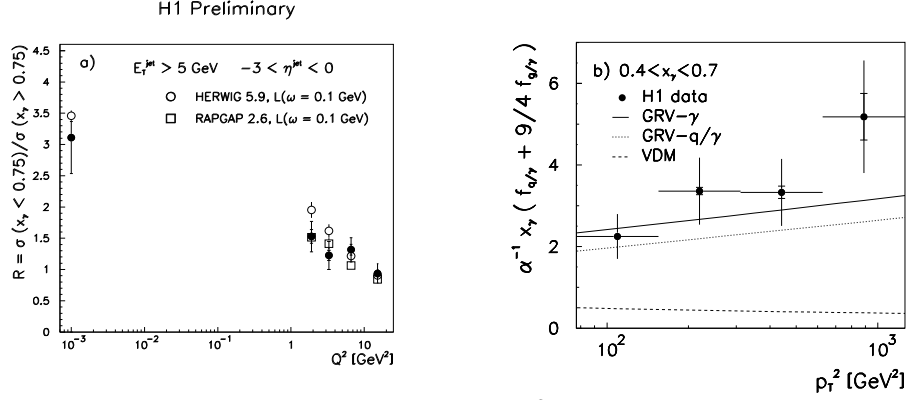


Figure 3: a) The ratio $\sigma_{res}/\sigma_{dir}$ as a function of Q^2 . The data (full circles) are compared to the HERWIG (open circles) and RAPGAP model (open squares) with DG suppression for $\omega = 0.1$ GeV. b) The LO effective PDF of the photon $x_\gamma f_{\text{eff}}^\gamma$ normalised to the α_{em} for $0.4 < x_\gamma < 0.7$ as a function of the squared parton momentum p_T^2 . The data (points) are compared to the pointlike (full curve), VDM (dashed) and quark (dotted) component of the effective GRV-LO PDF of the photon.

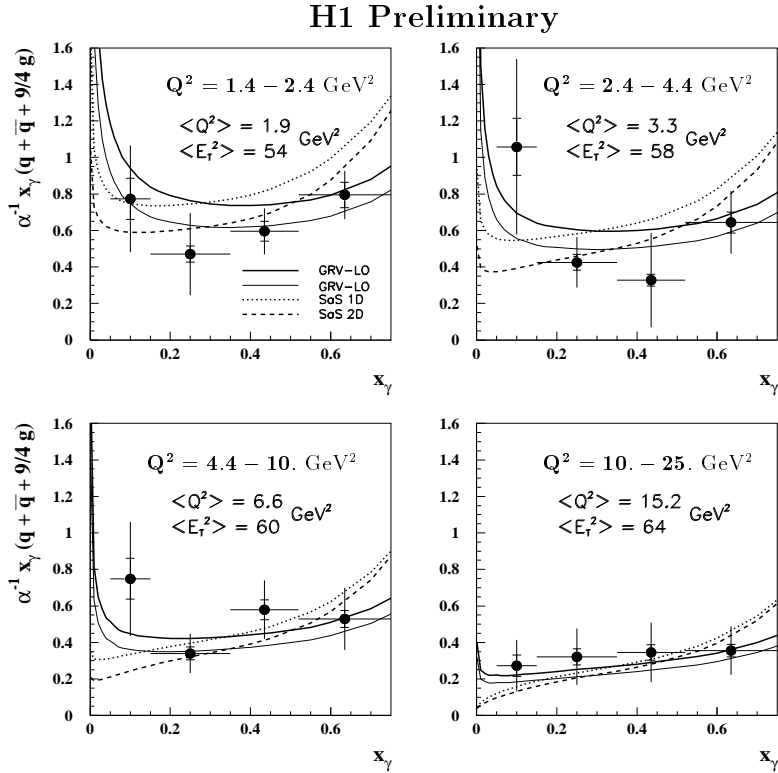


Figure 4: The LO effective parton distribution of the photon $x_\gamma f_{\text{eff}}^\gamma$, normalised to the α_{em} , in four intervals of the photon virtuality Q^2 . The data (points) are compared to the effective PDF of the photon using the GRV-LO parameterisation multiplied by DG suppression function with $\omega = 0.1, 0.05$ GeV (full thick, full thin line resp.) and SaS1D (dotted line), SaS2D (dashed line) parameterisations.